Hck/Fgr Kinase Deficiency Reduces Plaque Growth and Stability by Blunting Monocyte Recruitment and Intraplaque Motility

Indira Medina, PhD; Céline Cougoule, PhD*; Maik Drechsler, PhD*; Beatriz Bermudez, PhD; Rory R. Koenen, PhD; Judith Sluimer, PhD; Ine Wolfs, PhD; Yvonne Döring, PhD; Veronica Herias, PhD; Marjon Gijbels, PhD; Ilze Bot, PhD; Saskia C. A. de Jager, PhD; Christian Weber, MD; Jack Cleutjens, PhD; Theo J.C. van Berkel, PhD; Kees-Jan Sikkink, PhD, MD; Atilla Mócsai, PhD; Isabelle Maridonneau-Parini, PhD†; Oliver Soehnlein, PhD, MD†; Erik A.L. Biessen, PhD

***Background*—**Leukocyte migration is critical for the infiltration of monocytes and accumulation of monocyte-derived macrophages in inflammation. Considering that Hck and Fgr are instrumental in this process, their impact on atherosclerosis and on lesion inflammation and stability was evaluated.

***Methods and Results*—**Hematopoietic Hck/Fgr-deficient, LDLr$^{-/-}$ chimeras, obtained by bone marrow transplantation, had smaller but, paradoxically, less stable lesions with reduced macrophage content, overt cap thinning, and necrotic core expansion as the most prominent features. Despite a Ly6C^{high}-skewed proinflammatory monocyte phenotype, Hck/Fgr deficiency led to disrupted adhesion of myeloid cells to and transmigration across endothelial monolayers in vitro and atherosclerotic plaques in vivo, as assessed by intravital microscopy, flow cytometry, and histological examination of atherosclerotic arteries. Moreover, Hck/Fgr-deficient macrophages showed blunted podosome formation and mesenchymal migration capacity. In consequence, transmigrated double-knockout macrophages were seen to accumulate in the fibrous cap, potentially promoting its focal erosion, as observed for double-knockout chimeras.

***Conclusions*—**The hematopoietic deficiency of Hck and Fgr led to attenuated atherosclerotic plaque formation by abrogating endothelial adhesion and transmigration; paradoxically, it also promoted plaque instability by causing monocyte subset imbalance and subendothelial accumulation, raising a note of caution regarding src kinase–targeted intervention in plaque inflammation. **(*Circulation*. 2015;132:490-501. DOI: 10.1161/CIRCULATIONAHA.114.012316.)**

Key Words: immunology ■ atherosclerosis ■ cell migration assays ■ leukocytes ■ mobility ■ phosphotransferases ■ plaque, atherosclerotic

Inflammation and wound healing are determinants of disease progression and clinical outcome in atherosclerosis. They are emerging as interrelated processes with overlapping molecular mechanisms controlling monocyte infiltration and differentiation into macrophages, whose phenotype determines the stability of lesions, by controlling the balance between matrix degradation and inflammation versus matrix deposition and resolution of inflammation and wound healing.[1]

Clinical Perspective on p 501

Monocyte/macrophage intravasation is an essential step for metabolic disease pathogenesis including atherosclerosis. The ability of monocytes to roll and adhere to the endothelium in response to chemokines is crucial for macrophage accumulation.[2] It relies on actin-dependent morphological polarization, formation of filopodia and

Received October 1, 2012; accepted June 4, 2015.

From Experimental Vascular Pathology Group, Department of Pathology, CARIM, Maastricht University Medical Center, The Netherlands (I.M., J.S., I.W., V.H., M.G., J.C., E.A.L.B.); Division of Biopharmaceutics, Leiden Academic Center for Drug Research, Leiden University, The Netherlands (I.M., I.B., S.C.A.d.J., T.J.C.v.B.); CNRS, IPBS (Institut de Pharmacologie et de Biologie Structurale), Toulouse, France (C.C., I.M.-P.); Université de Toulouse, France (C.C., I.M.-P.); Institute for Prevention of Cardiovascular Prevention (IPEK), LMU Munich, Germany (M.D., R.R.K., Y.D., C.W., O.S.); Instituto de la Grasa, CSIC, Seville, Spain (B.B.); Department of Vascular Surgery, Orbis Hospital Sittard, The Netherlands (K.-J.S.); Department of Physiology; Semmelweis University, Budapest, Hungary (A.M.); Department of Pathology, Academic Medical Center (AMC), Amsterdam, The Netherlands (O.S.); and German Centre for Cardiovascular Research (DZHK), Munich Heart Alliance, Germany (O.S.).

*Drs Cougoule and Drechsler contributed equally.

†Drs Maridonneau-Parini and Soehnlein contributed equally.

The online-only Data Supplement is available with this article at http://circ.ahajournals.org/lookup/suppl/doi:10.1161/CIRCULATIONAHA.114.012316/-/DC1.

Correspondence to Erik A.L. Biessen, PhD, Maastricht University Medical Center, P. Debyelaan 25, 6229 HX Maastricht, The Netherlands. E-mail Erik.Biessen@maastrichtuniversity.nl

lamellipodia, binding of integrins to endothelial adhesion molecules, cytoskeletal reorganization,[3] and signal transduction pathways ultimately leading to the concerted loosening of adherent junctions on endothelial cells[4] and monocyte transmigration across endothelial, basement membrane, and fibrous cap barriers, before their homing in expanding lesions and differentiation into pro- or antifibrotic macrophages.

Hck and Fgr are 2 Src tyrosine kinases that display restricted coexpression in myeloid cells where they regulate β2-integrin binding to endothelial intercellular adhesion molecule-1 to facilitate cell adhesion and migration on P-selectin glycoprotein ligand-1 (PSGL-1) and CD44 interaction with endothelial E-selectin and P-selectin.[5,6] In addition, Hck and Fgr are a convergence point of signaling pathways initiated by a wide range of cell receptors implicated in the pathogenesis of atherosclerosis, including integrins, immune and growth factors, Fc-γ receptors (Fcγ) and chemokine receptors. These kinases exert their functions by the activation of several effectors including Rac/CDC42, spleen tyrosine kinase (Syk), and protein tyrosine kinase (PyK),[7] which are implicated in the accumulation and trapping of macrophages in atherosclerosis.[8–11] As expected from signaling molecules targeted by multiple receptors, Hck and Fgr mediate a broad spectrum of processes, ranging from cell proliferation, survival, and differentiation, to cytokine secretion, cytoskeleton dynamics, integrin-dependent cell adhesion, to the endothelium and migration.[7,12–15]

In light of these data, we hypothesized that Hck/Fgr deficiency would lead to reduced accumulation of macrophages in atherosclerosis onset and progression, a consequence of reduced diapedesis and migration. Our data imply that Hck and Fgr not only are progressively overexpressed in atherosclerosis, but they also control critical molecular processes in monocyte influx, blood monocyte subset balance, macrophage accumulation, and the maintenance of atherosclerotic lesion stability.

Materials and Methods

Animal Experiments

Bone marrow transplantation, perivascular collar placement, and intravital microscopy experiments were approved by the local regulatory authorities of Leiden and Maastricht, and performed in accordance with Dutch, French, and German government guidelines as described in the online-only Data Supplement Methods.

Cholesterol and Triglyceride Levels

Blood samples were taken by tail bleeding 1 day before and 5 weeks after the introduction of Western type diet (WTD) and at euthanization. Total plasma cholesterol, triglyceride, and phospholipid contents were measured by an enzymatic-colorimetric assay (Roche Diagnostics, Almere, The Netherlands).

Plasma Cytokine Levels

The Luminex 100 Bio-Plex cytokine assay (Bio-Rad Laboratories, Inc; Hercules, CA) was used to determine plasma levels of: interleukin (IL)-1α, IL-1β, IL-2, IL-4, IL-5, IL-6, IL-10, IL12(P40), IL-12(P70), IL-17, eotaxin, keratinocyte chemoattractant, monocyte chemoattractant protein-1, monocyte inflammatory protein-1α, and tumor necrosis factor-α (TNF-α). Statistical analysis was performed for the cytokines that reached the limit of detection (IL-1β, IL-12, eotaxin, monocyte chemoattractant protein-1, and IL-1α).

Blood Cell Analysis and Flow Cytometry

Blood, bone marrow, and peritoneal cells were harvested at euthanization, and single-cell suspensions were prepared. Lysis of erythrocytes was performed in ice-cold NH_4Cl (8.4 g/L), $NaHCO_3$ (1 g/L), and ethylenediaminetetraacetic acid (37 mg/L) during 3 minutes. Single-cell suspensions were stained with fluorescent label–conjugated antibodies for different markers and analyzed by fluorescence-activated cell sorting as detailed in the online-only Data Supplement Methods. Whole-blood samples were analyzed on a Sysmex blood cell analyzer (XT-2000i, Sysmex Europe GmbH, Norderstedt, Germany).

Cell Culture

Bone marrow–derived macrophages (BMDM) and peritoneal macrophages, vascular smooth muscle cells (SMC), human aortic endothelial cells, and Jurkat lymphocytes were cultured as detailed in the online-only Data Supplement Methods.

Thioglycolate-Induced Peritonitis

Cells were collected for analysis by fluorescence-activated cell sorting and microscopic quantification by Giemsa staining 1, 3, or 5 days (as indicated) after the induction of peritonitis with a sterile solution of dehydrated Brewer complete thioglycolate broth (1 mL, 2%–3% wt/vol, Difco Laboratories, West Molesy, UK).

Phagocytosis, Apoptosis, and Proliferation Assays

Proliferation and apoptosis assays, phagocytosis of apoptotic cells and zymosan particles, and cholesterol uptake experiments are detailed in the online-only Data Supplement Methods.

Macrophage Adhesion and Transmigration Across the Endothelium

Human aortic endothelial cells (PromoCell) were grown and preincubated with TNF-α (10 ng/mL) for at least 4 hours. Hck and Fgr mutant BMDM or wild-type (WT) controls were suspended at 5×10^5 cells/mL in 1× Hanks buffer, 20 mmol/L 4-(2-hydroxyethyl)-1-piperazineethanesulfonic acid, 0.5% human serum albumin (Baxter), and 1 mmol/L calcium and magnesium after stimulation with interferon-γ (IFN-γ; 100 U/mL Peprotech) during 16 hours. For the assessment of cell adhesion, macrophages were perfused over inflamed human aortic endothelial cell monolayers during 2 minutes at 0.1 mL/min and cells counted in 6 high-power field (100× magnification) pictures. Transmigration was recorded at a flow rate of 0.05 mL/min for 30 minutes in 15-second intervals by using a differential interference contrast microscope.

Macrophage Morphology, Migration, Podosome Rosette Formation, and Matrix Degradation

Assessment of macrophage morphology and 2- and 3-dimensional migration are detailed in the Methods in the online-only Data Supplement.

Gelatin Zymography and β-Hexosaminidase Release

Zymography experiments were performed as previously described.[13] In brief, BMDM (1×10^6 cells/well) were seeded overnight into 6-well fibronectin-coated plates. Conditioned cell culture medium and cell lysate were subjected to 10% (wt/vol) sodium dodecyl sulfate, 0.1 mg/mL gelatin gel electrophoresis. For β-hexosaminidase release, BMDM were seeded overnight into 6-well plates, the assay was performed on cell extracts obtained in 1% Triton X-100 and supernatants as previously described.[15]

Classical and Alternative Macrophage Polarization

BMDM (5×10^5 cells/well) were seeded in 24-well plates and allowed to adhere overnight before immune polarization was induced by

24-hour incubation with 100 U/mL IFN-γ (Peprotech) or 20 ng/mL IL-4 (Peprotech). RNA isolation, cDNA synthesis, and real-time polymerase chain reaction were performed as detailed in the online-only Data Supplement Methods.

SMC Collagen Synthesis and Proliferation

Cell proliferation, collagen, and noncollagenous protein extracellular deposition were assessed in vascular SMC layers by enzyme-linked immunosorbent assay (Roche, BrdU colorimetric kit) and a quantitative collagen and protein microassay kit (Chondrex, Inc, Redmond, WA), respectively, according to the manufacturers' instructions.

Tissue Harvesting, Immunohistochemistry, and Plaque Morphometry

Mice were anesthetized, euthanized, and perfused before the collection of hearts, aortas, common carotid arteries, peritoneal ascites, and other organs as described in the online-only Data Supplement Methods, which also contains a detailed description of cell and tissue staining and visualization procedures.

Analysis of Microarray Data

For microarray analysis, total RNA was extracted by using the guanidine thiocyanate/CsCl gradient method[17] and a NucleoSpin RNA II kit (Macherey Nagel, Duren, Germany), from early (n=13) and advanced stable (n=16) lesions obtained after autopsy (Department of Pathology, University Hospital Maastricht, Maastricht, the Netherlands) or advanced stable (n=21) and advanced unstable (n=23) lesions obtained on surgery (Department of Surgery, Maasland Hospital Sittard, Sittard, the Netherlands). RNA concentration and quality and lesion phenotype were determined as detailed in the online-only Data Supplement Methods. All human work was approved by the Ethics Committee of the University Hospital Maastricht. Written informed consent for participation in the study was obtained from all individuals. Samples from autopsy were individually hybridized to HGU133 2.0 Plus arrays (Affymetrix, Santa Clara, CA), and samples from surgery were individually hybridized to Illumina Human Sentrix-8 V2.0 BeadChip (Illumina Inc, San Diego, CA).

Microarray expression data of macrophage immune polarization were obtained at the Gene Expression Omnibus Web site (www.ncbi.nlm.nih.gov/geo) under accession number GSE18686.[18] Data normalization and summarization along with statistical, cluster, and Gene Ontology analysis are described in the online-only Data Supplement Methods.

Statistical Analysis of Experimental Data

Analyses were done using MatLab's Statistics ToolBox (Ver7.9) or INSTAT (Graphpad Software, Inc). Two-group comparisons were analyzed by the Welch Student *t* test to account for unequal variances (except for higher-powered data sets [n>8] with equivalent variance, where we opted for an unpaired *t* test). Two-sided *P* values of <0.05 were considered significant and denoted with 1, 2, or 3 asterisks when lower than 0.05, 0.01, or 0.001, respectively. Comparisons that did not reach significance were not highlighted by an asterisk.

Figure data are presented as mean±standard error of the mean (unless otherwise stated), whereas data in Results are given as relative change in comparison with the WT control. Regression lines were compared by analysis of covariance, using the independent variable plaque area as covariate and macrophage content or necrotic core size as outcome in a 2-group analysis of covariance. Linear regression slopes were plotted with 95% confidence intervals. Multiple comparison analyses were analyzed by 1-way analysis of variance with Bonferroni correction at a significance threshold of 0.05.

Results

Hematopoietic Deficiency in Hck and Fgr Reduces Atherogenesis

A first indication of the participation of the src kinases Hck and Fgr in atherosclerotic lesion progression was provided by their upregulation in advanced human atherosclerotic lesions in comparison with early ones (GSE28829; Figure IA in the online-only Data Supplement), whereas the expression of both kinases was also significantly increased in human atherosclerotic vulnerable lesions in comparison with stable ones (Figure IB in the online-only Data Supplement), linking them to lesion progression.

To establish active involvement of Hck and Fgr in atherosclerosis, we generated atherosclerosis-prone chimeric mice by reconstitution of lethally irradiated *LDLr*$^{-/-}$ recipient animals with *Hck*$^{-/-}$*Fgr*$^{-/-}$ double-knockout (dKO) or WT bone marrow cells. Hck/Fgr deletion did not lead to any alteration in total body weight along the experiment nor did it affect plasma total cholesterol levels before (199.4 mg/dL versus 150.8 mg/dL for WT controls) and after (1616.1 mg/dL versus 1488.9 mg/dL, for WT controls) WTD introduction. Plasma levels of proinflammatory cytokines such as IL-1β, IL-12, eotaxin, monocyte chemoattractant protein-1, and IL−1α, as measured at euthanization, were not influenced by Hck/Fgr deficiency (Figure IC in the online-only Data Supplement).

WTD-fed chimeric mice transplanted with Hck/Fgr dKO bone marrow exhibited 30% ($P \leq 0.05$) reduction in intermediate atherosclerotic lesion size (Figure 1A), whereas, at later stages of plaque progression, it led to 40% smaller plaques ($P \leq 0.01$; Figure 1B and 1C). Unexpectedly, despite their reduced size, plaques from Hck/Fgr dKO chimeras exhibited a more vulnerable plaque phenotype, characterized by necrotic core expansion (+68%; $P \leq 0.01$; Figure 1D) and significant reductions in collagen and SMC (–75% and –82%, respectively, both $P \leq 0.001$; Figure 1E and 1F) and fibrous cap thickness (–53%, $P \leq 0.001$; Figure 1G and 1H). The apoptotic rate in early lesions, as measured by caspase-3 staining, did not differ between dKO versus WT chimeras (Figure 1I). The diminished plaque fibrosis was coupled with 34% ($P \leq 0.001$; Figure 1J and 1K) and 61% ($P \leq 0.05$; Figure 1L and 1M) reductions in intimal macrophage and adventitial neutrophil contents, respectively. Because plaque cell proliferation, assessed by Ki67 staining, was unchanged (Figure 1N), it is unlikely that the reduced plaque macrophage content results from Hck/Fgr deficiency–associated effects on plaque macrophage expansion. Statistical regression analysis revealed that, although necrotic core size and plaque macrophage content were both associated with plaque size ($P \leq 0.001$ for both), neither of the 2 did so in a genotype-dependent manner, indicating that the changes in plaque macrophage content and necrotic core size reflected a delayed plaque progression (Figure ID and IE in the online-only Data Supplement). The reduced presence of (F4/80^{+}) plaque macrophages in dKO versus WT chimeras was confirmed by flow cytometry analysis of aorta (–42%, $P \leq 0.001$), whereas vascular CD3^{+}-T lymphocyte content was unchanged (Figure 2A and 2B). This aligns well with the observation that Hck and Fgr showed highest expression in myeloid cells at mRNA (Figure 2C) and protein level, as well (Figure 2D).

To address whether the diminution of plaque macrophage and neutrophil numbers was caused by a reduced availability of myeloid subsets in dKO chimeras, we studied the impact of Hck/Fgr deficiency on myeloid versus nonmyeloid subset patterns in blood, spleen, and bone marrow. The absolute and

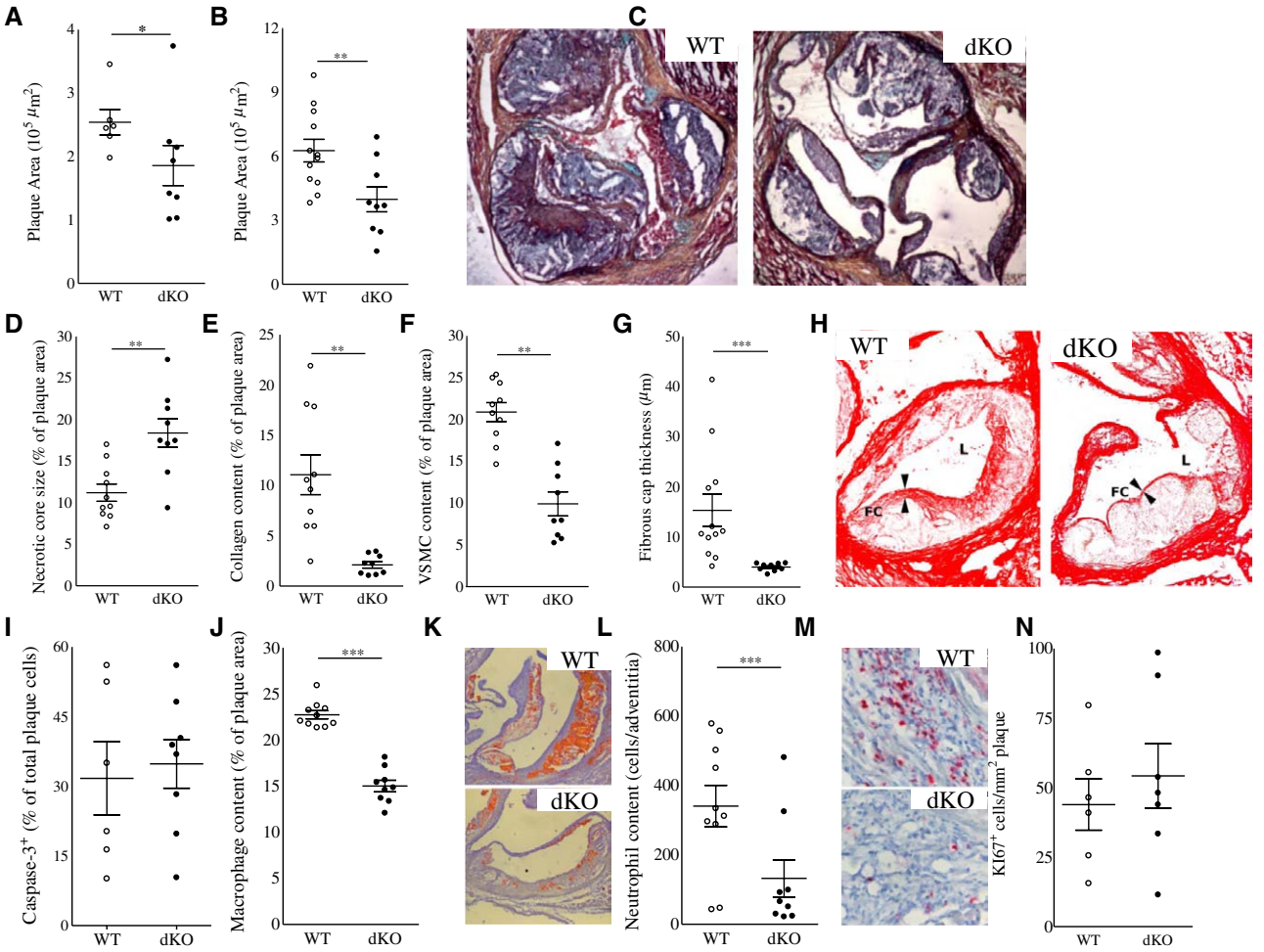

Figure 1. Reduced lesion size and altered lesion composition in Hck/Fgr dKO chimeras. Hck/Fgr deficiency led to reduced formation of intermediate (–29%, n=8, 10 sections analyzed per unit; **A**) and advanced lesions (–37%, n=13, 10 sections per unit; **B**) in aortic roots of Western type diet–fed LDLr$^{-/-}$ mice. **C**, Representative Movat-stained advanced plaque sections. Advanced lesions from Hck/Fgr dKO chimeras displayed features of plaque vulnerability characterized by bigger necrotic cores (+68%; **D**), reduced collagen (–82%; **E**), reduced SMC (–75%) contents (**F**), and thinner fibrous caps (–53%; **G**; n=13, 6 sections per experimental unit). **H**, Representative pictures corresponding to **D** through **G** denoting lumen size (L), necrotic core (NC) expansion, fibrous cap (FC) thinning, and diminished collagen area (Picrosirius Red staining in dKO chimeras). **I**, Lesion caspase 3$^+$ cell content was unchanged in Hck/Fgr deficiency. Intimal macrophages (**J** and **K**) and adventitial neutrophils (**L** and **M**), were reduced by 34% and 61%, respectively, in advanced lesions. **K** and **M** display representative slides of macrophage and neutrophil stainings, respectively. Lesions of dKO mice showed similar Ki67$^+$ cell content, reflecting unchanged proliferation (**N**). WT, open circles; dKO, filled circles; *P≤0.05, **P≤0.01, ***P≤0.001. dKO indicates double-knockout; SMC, smooth muscle cells; and WT, wild type.

relative levels of circulatory, bone marrow, and spleen white blood cells, T (cytotoxic, helper, and Tregs) and B lymphocytes, and spleen dendritic cells (resident and plasmacytoid), as well, were not disturbed in WTD-fed dKO chimeric mice (data not shown) in comparison with WT controls. Similarly, equivalent myeloid cell composition (Figure IIA in the online-only Data Supplement) and monocyte subset levels (Figure IIB in the online-only Data Supplement) were observed in bone marrow. Expression of Ly6C was not influenced by lack of Hck/Fgr in Ly6C^{low} and Ly6C^{high} blood monocyte subsets. This suggests that the increased Ly6C is not attributable to the deficiency of Fgr, which was seen to bind Ly6C and activate LFA-1[19] (Figure IIC and IIE in the online-only Data Supplement). Similarly, absolute or relative levels of circulatory granulocytes and monocytes were unchanged (Figure IIF through III in the online-only Data Supplement). Relative Ly6C^{high} monocyte abundance (+47%, P≤0.01), however, was significantly increased (Figure IIJ in the online-only Data Supplement), which generally is thought to be associated with increased invasion into atherosclerotic lesions. Nevertheless, significantly fewer leukocytes (Figure 2E) and, in particular, fewer monocytes/macrophages (Figure 2F and 2G) were recruited to the peritoneal cavity of dKO chimeras in a model of thioglycolate-induced peritonitis. The expression of monocyte chemotaxis mediating chemokine receptors (CCR2, CCR5, CXCR1-3, and CX_3CR1) by sorted Ly6C^{high} bone marrow monocytes was unchanged (Figure IF in the online-only Data Supplement); likewise, dKO macrophages did not display altered expression of chemokines CCL2 and CCL5 (Figure IG in the online-only Data Supplement). This suggests that the reduced macrophage invasion into inflamed peritoneum or plaque is not attributable to aberrant chemotaxis. No differences in the activation of macrophages were observed, as assessed by the expression of CD86, CD40, and

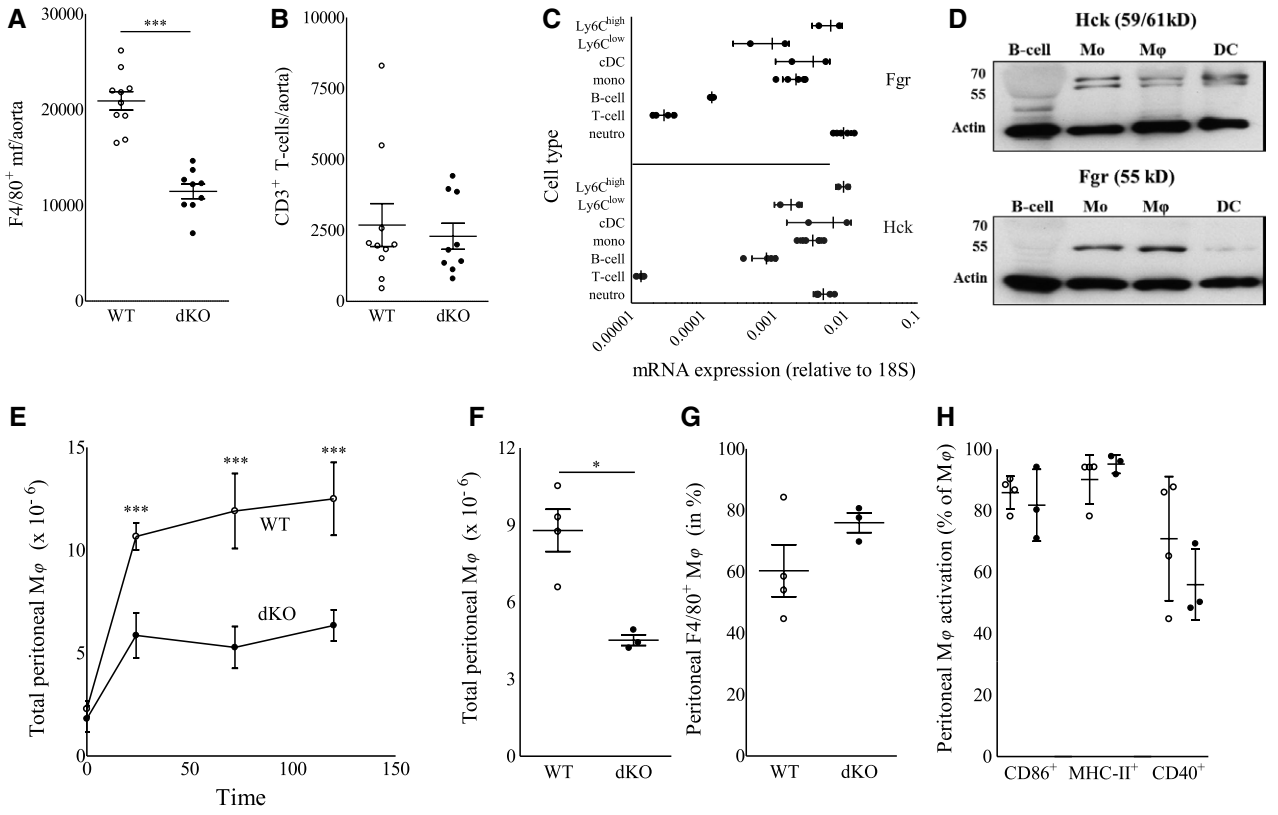

Figure 2. A and **B**, Flow cytometry analysis of aorta-associated leukocytes in Hck/Fgr dKO vs WT bone marrow–transplanted LDLr$^{-/-}$ mice. Hck/Fgr deficiency was associated with a reduced accumulation of F4/80^{+} macrophages (**A**) but had no effect on CD3+ lymphocyte contents (**B**) of aortas of WTD-fed LDLr$^{-/-}$ mice. WT, open circles; dKO, filled circles; ***P≤0.001 (n=9). **C** and **D,** Expression analysis established myeloid cell–specific expression of Hck and Fgr. C, Hck (**top**) and fgr (**bottom**) mRNA expression by monocytes (total, Ly6C^{high}, and Ly6C^{low}), cDC, neutrophils B cells and T cells isolated by FACS from total spleen of WT and dKO chimeras; expression values are expressed relative to that of 18S (mean±SD; n=4). **D**, Specific expression of Fgr (**bottom**) and Hck (**top**) by monocytes and macrophages, but not B cells and dendritic cells (Fgr), was confirmed at protein level by Western blot analysis for Hck (59/61 kDa) and Fgr (55 kDa). Arrows indicate the position of 70- and 55-kDa calibration markers. β-Actin served as loading control. **E** through **H,** Reduced thioglycolate induced peritonitis in Hck/Fgr-deficient mice. **E**, The absolute levels of inflammatory cells recruited to the peritoneal cavity was reduced in dKO chimeras 24, 72, and 120 hours after intraperitoneal injection of thioglycolate. **F**, Absolute monocyte/macrophage counts in peritoneal ascites were reduced by 48.5% 120 hours after the induction of peritonitis in dKO chimeras. **G**, Relative monocyte/macrophage numbers in the peritoneal cavity were unchanged. **H**, The expression of activation markers was not perturbed by the lack of Hck/Fgr (n=6, duplicated samples per experimental unit). WT, open circles; dKO, filled circles; *P≤0.05, ***P≤0.001. cDC indicates conventional dendritic cell; dKO, double-knockout; FACS, fluorescence-activated cell sorting; SD, standard deviation; WT, wild type; and WTD, Western type diet.

major histocompatibility complex II (Figure 2H), indicating that Hck/Fgr deficiency did not perturb the activation potential of macrophages, a result that could be relevant for atherosclerotic lesion macrophages.

Lack of Hck/Fgr Leads to Reduced Leukocyte Adhesion to the Endothelium

Echoing the reduced accumulation of dKO macrophages in peritonitis and atherosclerotic lesions, we found that adoptively transferred fluorescently labeled dKO BMDM displayed profoundly reduced adhesion (–67%, P≤0.001) and almost ablated transmigration (–88%; P≤0.001) to preexisting collar-induced carotid artery lesions induced in WTD-fed *LDLr*$^{-/-}$ mice (Figure 3A through 3C). Next, we performed intravital microscopy analysis at the carotid artery bifurcation of WTD-fed WT versus dKO chimeras after in situ labeling of circulating leukocytes (Rhodamine G or Rho), CD11b^{+} monocytes, CD11b^{+} Ly6C^{high} monocytes, and Ly6G^{+} neutrophils. Concordant with the aforementioned adoptive transfer studies, plaque neutrophil and monocyte adhesion were sharply reduced (P≤0.001 for all; Figure 3D and 3E), at which the effects on CD11b^{+} Ly6C^{high} monocytes seemed to be most pronounced. Extending this finding, we sought to track the dynamics and more, in particular, the plaque-homing capacity of proinflammatory LyC6^{hi} monocytes in WT versus Hck/Fgr-deficient mice. Hereto, we used the Ly6C^{high} monocyte-specific latex labeling procedure described by Tacke et al[20] and observed reduced amounts of latex bead–laden Ly6C^{high} cell–derived macrophages in plaque 24 hours after bead labeling as witnessed in flow cytometry and fluorescent microscopy analysis (Figure 3F through 3H).

To be able to dissect the individual steps in monocyte recruitment to the plaque, we performed flow experiments. dKO BMDM perfused through a monolayer of inflamed endothelium in vitro displayed reduced adhesion (–52%; P<0.05; Figure 4A and 4B). However, the percentage of adherent cells able to transmigrate across the endothelium in vitro was not influenced by Hck/Fgr deficiency (Figure 4C), implying that

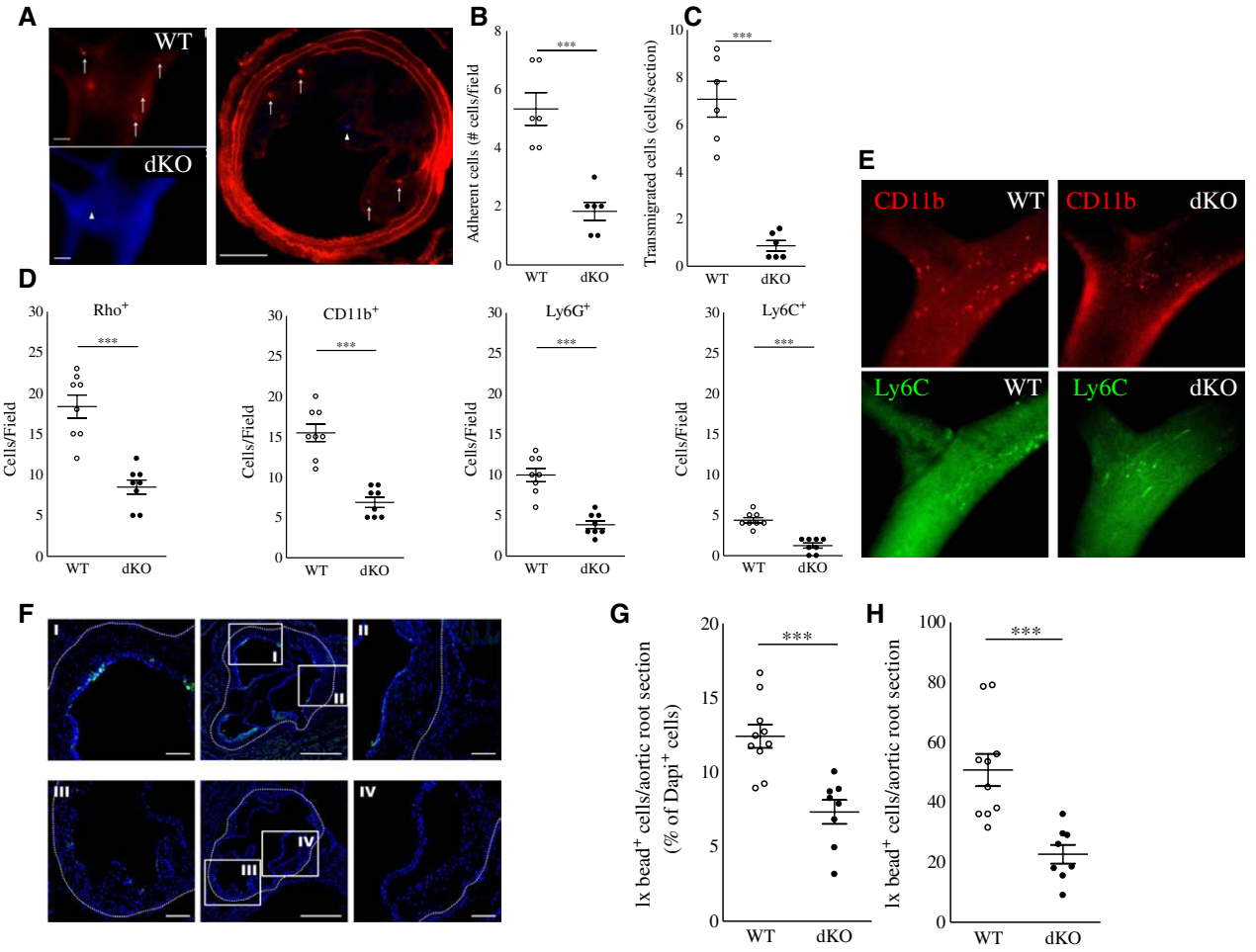

Figure 3. Impaired adhesion to the endothelium and transmigration of Hck/Fgr-deficient macrophages in vivo. **A** through **C,** DAPI-labeled Hck/Fgr dKO and DiI-labeled WT BMDM adoptively transferred to atherosclerotic LDLr$^{-/-}$ mice (10^6 BMDM/genotype/mouse) displayed reduced adhesion to (**A** and **B**) and transmigration (**A** and **C**) into preexisting atherosclerotic lesions induced by perivascular collar placement. Hck/Fgr dKO (arrowheads, blue) and DiI-labeled WT (arrows, red) BMDM are shown to adhere and home to the central atheroma 15 minutes (**A**, **left**, intravital microscopy) and 1 day (**A**, **right,** postmortem section) after cell cotransfer (scale bar, 100 μm). **D**, Circulating leukocytes in atherosclerotic WT vs dKO bone marrow–transplanted LDLr$^{-/-}$ with were labeled in situ with Rhodamine 6G (Rho), while, in a parallel experiment, monocyte subsets and neutrophils were labeled with fluorescently tagged CD11b, Ly6C, and Ly6G antibodies immediately before intravital microscopy analysis at the carotid artery bifurcation (**D**; n=8). dKO chimeras clearly show reduced adhesion of Rho$^+$ myeloid cells, CD11b$^+$ (all) monocytes, CD11b$^+$ Ly6C^{high} monocytes, and Ly6G$^+$ neutrophils (**D**). **E**, Representative intravital microscopy images of monocyte adhesion in WT vs dKO chimeras (red: CD11b, green Ly6C). Circulating Ly6C^{high} monocytes were selectively labeled with fluorescent latex beads 72 hours after clodronate liposome–induced depletion of circulating monocytes in dKO and WT bone marrow–transplanted LDLR$^{-/-}$ mice. Fluorescent microscopy analysis of aortic arch plaques 24 hours after bead injection showed a reduced presence of bead-laden macrophages in plaques of dKO chimeras (**F**, Central panels represent overview, I and II are high-power views detailing for WT mice, whereas III and IV are high-power views of dKO mice; n=9). Quantitative analysis of plaques confirmed significant reductions in Ly6C^{high} monocyte influx, both at relative (**G**) and absolute (**H**) level. WT, open circles; dKO, filled circles; *P≤0.05, **P≤0.01, ***P≤0.001. BMDM indicates bone marrow–derived macrophages; DAPI, 4′,6-diamidino-2-phenylindole; DiI, 1,1'-dioctadecyl-3,3,3',3'-tetramethyl-indocarbocyanine perchlorate; dKO, double-knockout; and WT, wild type.

the inhibited transendothelial macrophage migration mainly reflects the previous impairment of the adhesion mechanism.

This intriguing observation led us to investigate the (trans) migration process in closer detail. In vitro, dKO BMDM displayed almost ablated wound invasion in a wound healing assay (–94%, P≤0.001; Figure 4D), despite that proliferation rates under baseline and lipopolysaccharide (LPS)-stimulated conditions (Figure IIIA in the online-only Data Supplement) and seeded cell densities were similar in both genotypes, indicating impaired 2-dimensional migration. In addition, dKO peritoneal macrophages presented altered morphology in vitro characterized by lack of elongation (–56%, P≤0.001) and morphological polarization (P≤0.001), whereas the cells were also featuring sharply reduced filopodium and lamellipodium formation (Figure 4E through 4I), which is suggestive of dysfunctional actin network polymerization.

Taken together, these results indicate impaired adhesion and 2-dimensional crawling on the endothelium previous to diapedesis, as contributing factors to the reduced macrophage accumulation observed in atherosclerotic dKO chimeras.

Hck/Fgr-Deficient Macrophages Display Reduced 3-Dimensional Migration

We next assessed the 3-dimensional migration capacity of dKO macrophages, taking into account that, in particular, at later stages of lesion progression, extravasated cells must pass

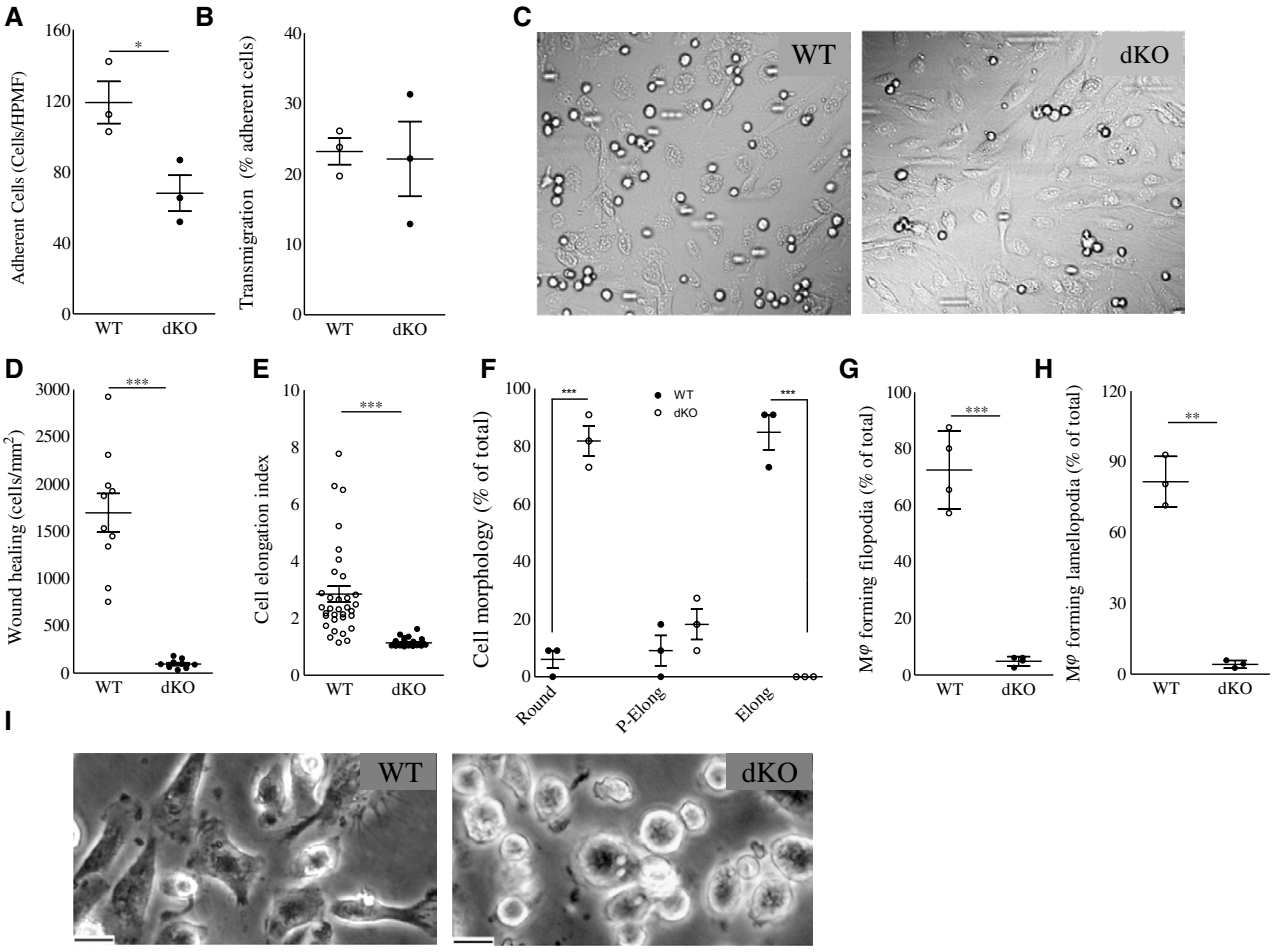

Figure 4. Hck/Fgr dKO macrophages display impaired 2-dimensional directional migration and aberrant morphology. Adhesion (**A**) but not transmigration (**B**) across monolayers of inflamed endothelium in vitro is reduced in dKO BMDM (n=3, 6 high-power microscopic field [HPMF] quantifications per sample). **C**, Representative differential interference contrast microscopy HPMF pictures of BMDM adherent to inflamed endothelium in vitro. **D**, dKO macrophages display 94% reduced 2-dimensional migration and wound healing capacity in vitro (n=3, 5 area quantifications per replicate). **E** and **F**, Morphology of peritoneal macrophages (PEM) cultured for 36 hours (n=5, 100 cells per replicate). **E**, Mean elongation index (EI, defined as the ratio of cell length to cell breadth). **F**, Percentage of rounded (EI<1.2), partially elongated cell (1.2<EI<2) and elongated (EI>2) and as judged by the EI. **G** and **H,** Percentage of PEM cultured for 16 hours, forming filopodia (**G**) and lamellipodia (**H**; n=5, 100 cells per replicate). **I**, Representative pictures depicting rounded cell morphology in dKO in comparison with WT PEM (Scale bar, 10 μm). WT, open circles; dKO, filled circles; **P*≤0.05, ****P*≤0.001. BMDM indicates bone marrow–derived macrophages; dKO, double-knockout; and WT, wild type.

through collagen and SMC-rich fibrous caps. Macrophages use mesenchymal and amoeboid migration mechanisms to perform 3-dimensional infiltration[21] either by protease-dependent degradation of dense extracellular matrices or by squeezing and deforming their cell body into extracellular matrix pores, respectively. In vitro, dKO BMDM displayed unimpeded amoeboid migration across type I fibrillar collagen (Figure 5A), which contrasted with their markedly inhibited mesenchymal migration through dense Matrigel (Figure 5B). Furthermore, the addition of a cocktail of protease inhibitors inhibited the mesenchymal migration through Matrigel in WT BMDM to levels observed in untreated mutant cells. However, it failed to impact the migration capacity of mutant BMDM (Figure 5B). This suggests that Hck/Fgr deficiency–associated ablation of mesenchymal migration implicates protease activity. Next, we examined whether dKO BMDM display abnormal secretion of proteases. The release of the lysosomal hydrolase β-hexosaminidase (Figure 5C), and of metalloproteinases 2 and 9, as well, was not affected (Figure 5D) however, excluding vesicular secretion defects to have underlain the observed impairment of macrophage migration.[21]

The mesenchymal migration of macrophages requires cell adhesion and extracellular matrix–degrading structures called podosomes.[22–24] As we already have shown, macrophage podosome stability and function are regulated by Hck in macrophages.[13,16] BMDM from WT mice formed large podosome rosettes; dKO cells, in contrast, formed fewer and smaller podosome rosettes (Figure 5E and 5F). As a consequence, focal extracellular matrix degradation capacity of dKO macrophages as assessed by fluorescein isothiocyanate gelatin degradation, was significantly decreased in comparison with their WT counterpart (Figure 5G and 5H).

Taken together, these results indicate that Hck/Fgr gene deletion causes reduced mesenchymal migration by impairing the formation of podosome rosettes leading to diminished pericellular degradation of the extracellular matrix. This potentially has major implications for the invasive capacity of extravasated plaque macrophages. Therefore, we have histologically

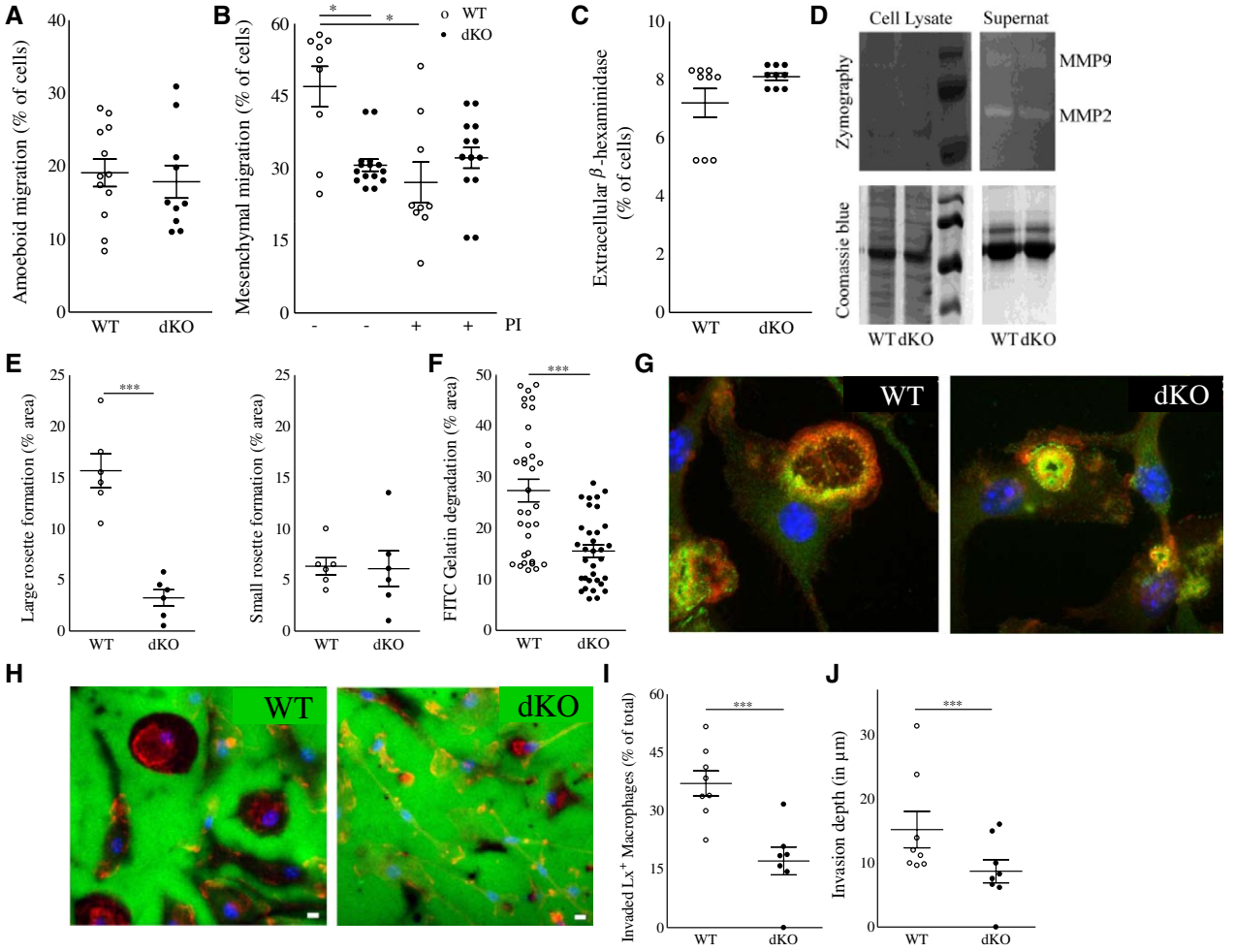

Figure 5. Hck/Fgr-deficient macrophages have impaired 3-dimensional migration capacity in vitro and in vivo. Hck/Fgr-deficient BMDM displayed normal amoeboid (mean±SEM of n=12; **A**) but reduced mesenchymal migration across Matrigel transwells where proteinase inhibitors (PI) inhibited WT but not dKO BMDM migration (mean±SEM; n=9–13; **B**). **C**, β-Hexosaminidase was released at similar levels in WT and dKO BMDM (mean±SD of n=3, in triplicate). **D**, Metalloproteinases MMP-2 and MMP-9 secretion, assessed by gelatin zymograph, is unaffected in dKO BMDM. **E,** dKO BMDM form less and smaller podosome rosettes than WT controls (n=5). Representative graphs illustrating large podosome rosettes (**left**) in WT BMDM and small podosome rosettes (**right**) in dKO BMDM, 100× magnification. **F**, FITC-gelatin degradation is reduced in dKO BMDM (n=3). **G** and **H**, Representative pictures of BMDM showing fewer and smaller gelatin proteolysis areas (in dark) colocalizing with podosome rosettes in dKO BMDM in comparison with WT controls (blue for cell nuclei, red for F-actin in **F** and **H**, green for Vinculin in **F**, and FITC-gelatin in **H**). Likewise, reinspection of the in vivo latex bead–aided monocyte/macrophage tracking experiment showed that 24 hours after labeling the portion of latex bead$^+$ plaque contained macrophages that had invaded into the atheroma (defined as located at >3 µm from the endothelium) was significantly reduced in dKO chimeras (n=8; **I**), whereas also the average plaque invasion depth of latex$^+$-labeled macrophages was seen to be reduced in these mice (**J**). WT, open circles; dKO, filled circles; *P≤0.05, **P≤0.01, ***P≤0.001. BMDM indicates bone marrow–derived macrophages; dKO, double-knockout; FITC, fluorescein isothiocyanate; Lx+, latex+; SEM, standard error of the mean; and WT, wild type.

reinspected the plaque for the presence and location of latex bead–labeled cells in the monocytes/macrophages tracking study described in Figure 3. In keeping with the impaired mesenchymal migration capacity in vitro, we observed that significantly less latex$^+$ macrophages had migrated beyond the basal membrane into the plaque atheroma (–58%, P<0.001; Figure 5I). Moreover, the average invasion depth of latex$^+$ macrophages that had invaded into the plaque at 24 hours after labeling was sharply reduced as well (–77%; P≤0.01; Figure 5J).

Hck/Fgr-Deficient Macrophages Display Impaired Efferocytosis and an Antifibrotic Phenotype

The subendothelial accumulation of macrophages could have contributed to the more vulnerable phenotype of dKO chimeras versus their WT counterparts, as hallmarked by reduced fibrosis and cap thinning. Because features of plaque vulnerability are often associated with disbalanced extracellular matrix homeostasis, owing to the proinflammatory, collagen synthesis inhibitory, and erosive milieu presented by plaque macrophages, in particular, if polarized toward a classically activated phenotype.[1] Moreover Ly6C^{high} monocytosis, as observed in dKO chimeras (Figure IIJ in the online-only Data Supplement), by itself has already been linked to preferential polarization toward classically activated macrophages.[25]

Therefore, we investigated whether Hck/Fgr deficiency has impacted macrophage phenotype. We first assessed whether macrophage polarization itself influences Hck/Fgr expression by transcriptome analysis of differentially expressed genes

from human macrophages stimulated with TNF-α, IL-4, IL-17, LPS, IFN-γ, or LPS+IFN-γ (GSE18686[18]). Hck and Fgr are included in separate gene networks, as revealed by K-means cluster analysis (C-IV and C-III, respectively; Figure 6A). Principal component analysis indicated that C-III and C-IV contained genes with upregulated expression in response to alternative (IL-4) and classic (LPS, IFN-γ, or LPS+IFN-γ) stimulants, respectively (Figure 6B). Consistently, Hck and Fgr were more than 2-fold upregulated in response to IFN-γ and IL-4, respectively (Figure 6C), suggesting their divergent participation in classic and alternatively activated macrophage molecular networks, respectively. This was confirmed at the protein level by Western blotting on naïve and primed BMDM from WT and dKO mice, showing a tendency toward increased Hck expression by classically activated macrophages and increased Fgr by alternatively activated macrophage (Figure 6D and 6E). Although conclusive evidence is lacking, classically activated macrophages are believed to represent the dominant phenotype in plaque. This therefore implies a major role for Hck in plaque macrophage function, as also suggested by the upregulation of Hck in advanced rupture-prone human atherosclerotic lesions (Figure IA and IB in the online-only Data Supplement)

However, the analysis of polarization marker gene expression failed to demonstrate consistent Hck/Fgr deficiency–associated changes in macrophage phenotype. Baseline mRNA

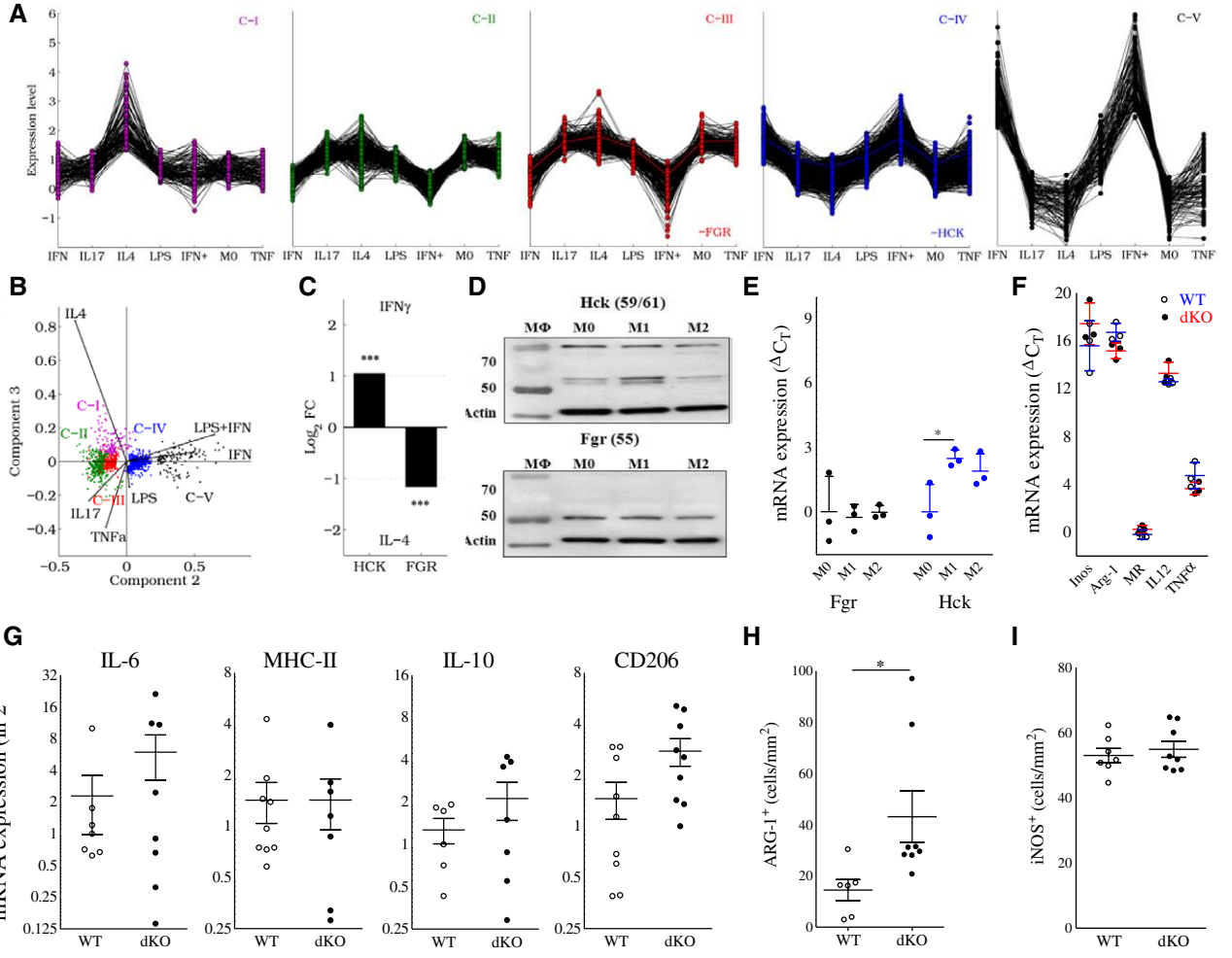

Figure 6. Hck/Fgr are involved in separate macrophage polarization programs, but their combined deficiency does not impact polarization marker expression. **A**, K-means clustering of human genes modulated on stimulation with IFN-γ, IL-17, IL-4, LPS, IFN-γ +LPS (denoted as IFN+) or TNF-α generates 5 clusters (C-I to C-V). Fgr and Hck belong to C-III and C-IV, respectively, and display opposite expression patterns. **B**, Principal component analysis (PCA) of modulated genes; 99.3% of the variance of the system lies within the first 3 principal components (PC1:84.8, PC2:13.2, and PC3:1.3%). **C**, Human Hck and Fgr expression is upregulated in response to IFN-γ and IL-4, respectively. **D**, This finding was confirmed by Western blotting on BMDM of WT vs dKO mice cultured in the absence (M0) or presence of IFN-γ (100 U/mL, M1) or IL-4 (20 ng/mL, M2; n=3). Quantification of Fgr (black symbols) and Hck (blue symbols) protein band intensities, corrected for the actin-loading control (mean±SD; n=3) is depicted in **E**. **F**, mRNA expression of classical (iNOS [inducible nitric oxide synthase]; IL-12; TNF-α) and alternatively activated macrophage markers (Arg-1, arginase-1; MR, mannose receptor) in nonstimulated BMDM in vitro as assessed by qPCR was not affected. Relative expression was calculated using cyclophilin as a housekeeping gene. qPCR data are presented as RE+$2^{-(\Delta\Delta Ct-SD\Delta\Delta Ct)}$ and RE-$2^{-(\Delta\Delta Ct+SD\Delta\Delta Ct)}$, mean±SD; n=3–4). qPCR of mRNA isolated from aorta of atherosclerotic LDLr$^{-/-}$ mice transplanted with WT and dKO bone marrow did not reveal any differences in expression of IL-6 (M1), MHC-II (M1) and IL-10 (M2), whereas that of CD206 (M2) was increased (**G**; n=6); in agreement, immunohistochemical analysis of aorta plaques showed slightly increased arg-1 (**H**), but unchanged iNOS staining (**I**; n=6–8). WT, open circles; dKO, filled circles. BMDM indicates bone marrow–derived macrophages; dKO, double-knockout; IFN-γ, interferon γ; LPS, lipopolysaccharide; MHC-II, major histocompatibility complex II; qPCR, quantitative polymerase chain reaction; TNF-α, tumor necrosis factor-α; and WT, wild type.

expression of established classically activated macrophage markers by nonstimulated BMDM such as inducible nitric oxide synthase, IL-12, or TNF-α was essentially unchanged, as was that of the alternatively activated macrophage markers arginase-1 and the mannose receptor (Figure 6F). Likewise, polarization marker gene expression by LPS+IFN-γ or IL-4–primed WT and dKO BMDM were largely similar (Figure IIIB and IIIC in the online-only Data Supplement, respectively). At the protein level, dKO and WT BMDM showed equivalent IL-12 secretion, whereas TNF-α production was slightly increased (Figure IIID in the online-only Data Supplement) and that of nitric oxide was significantly reduced (Figure IIIE in the online-only Data Supplement). Concordant with these data, mRNA expression analysis on isolated aorta did not reveal major changes in macrophage polarization marker expression pattern, apart from a slight increase in CD206 expression (Figure 6G), whereas inducible nitric oxide synthase$^+$ and arg-1$^+$ macrophage content in intermediate lesions did not point to a shift toward classical macrophage activation in dKO versus WT chimeras either (Figure 6H and 6I).

Because the complexity of macrophage adaptive responses in vivo cannot be completely captured by the rigid dichotomy of the macrophage polarization model in vitro, we focused on Src kinase–associated differences in macrophage functions that could underlie dKO-associated plaque destabilization. First, we assessed whether Hck/Fgr deficiency impacts macrophage cell death or their ability to ingest particles, opsonized particles, and cholesterol accumulation, functions that are potentially controlled by src kinases and are relevant to plaque stability. Hck/Fgr-deficient BMDM exposed normal apoptotic susceptibility (Figure IVA in the online-only Data Supplement), phagocytosis of fluorescent latex beads or opsonized particles (Figure IVB and IVC in the online-only Data Supplement), and uptake of modified cholesterol, in vitro, as assessed by high-performance thin layer chromatography or fluorescent microscopy (Figure IVD and IVE in the online-only Data Supplement). Efferocytosis, defined as the macrophage capacity to process apoptotic cells, however, was considerably reduced in dKO BMDM (Figure IVF in the online-only Data Supplement), which could at least in part explain the necrotic core expansion observed in dKO chimeras.

Interestingly, incubation of vascular SMC with conditioned medium from nonstimulated dKO BMDM did not influence their proliferation (Figure VA in the online-only Data Supplement), but reduced their deposition of extracellular collagen and noncollagenous proteins akin to conditioned medium from LPS-primed WT macrophages and starvation medium (Figure VB and VC in the online-only Data Supplement). Apparently, Hck/Fgr deficiency favors a macrophage antifibrotic differentiation phenotype, and we propose that the impact of this effect will even be amplified by the reduced mesenchymal migration into the plaque of dKO macrophages, conducive to increased focal accumulation of antifibrotic macrophages in close proximity to the fibrous cap.

Discussion

Here, we present conclusive evidence that Hck/Fgr deficiency leads to reduced atherosclerotic lesion burden with concomitant reductions in macrophage accumulation and, paradoxically, lesion stability. As we show, the former is attributable to impaired adhesion of macrophages to the endothelium, whereas the latter is likely attributable to blunted mesenchymal migration into the plaque atheroma, resulting in the retention of lytic macrophages in the plaque's fibrous cap.

As a first hallmark of Hck/Fgr deficiency, atherosclerotic lesions displayed reduced amounts of macrophages despite the marked skewing of monocyte differentiation toward a Ly6C^{high} phenotype, a subset known for its hypermigratory and proinflammatory profile and selective accumulation in atherosclerosis.[20,25]

With the use of intra- and extravital microscopy analysis of fluorescent dye, antibody and latex bead–labeled leukocyte subsets, we were able to firmly establish Hck/Fgr deficiency–induced impairment of monocyte and neutrophil adhesion to and diapedesis into plaque, while their chemotactic profile remained unaffected. This finding was confirmed by post hoc immunohistochemical analysis of plaque for the presence of latex bead–laden macrophages. The reduced presence of (Ly6C^{hi}) monocyte–derived macrophages is especially remarkable given the relative abundance of circulating Ly6C^{high} monocytes in dKO chimeras. This subset is thought to be associated with higher Ly6C^{high} monocyte infiltration[20,25] and reduced accumulation of profibrotic and anti-inflammatory macrophages.[26] It should be noted, however, that the Ly6C^{low} subset has been shown to contribute to plaque inflammation at later stages of disease development and has repeatedly been linked to plaque vulnerability and fibrosis.[27–29]

In addition, Hck/Fgr-deficient macrophages featured an impaired morphological polarization and disrupted 2-dimensional migration. dKO macrophages were unable to form filopodia and lamellipodia, which is critical for those cells to adhere and establish leading and trailing poles that direct their mobilization toward higher concentrations of chemoattractants.[30] Taken together, these results imply that Hck/Fgr deficiency results in reduced adhesion and directional crawling on the endothelium and, therefore, in impaired extravasation of circulating monocytes into the atherosclerotic lesion. The 3-dimensional mesenchymal migration of macrophages depends on the formation of podosome rosettes, which release proteolytic enzymes to perform pericellular degradation of the extracellular matrix.[21] In vitro, dKO macrophages exhibited an attenuated focal degradation of extracellular matrix, disrupted formation of podosome rosettes, and accordingly disrupted mesenchymal migration. Extrapolating these findings to atherosclerosis, Hck/Fgr deficiency has impacted both the adhesion of monocytes to the plaque and their mesenchymal migration across the lesional fibrous cap, as well, contributing to the striking reduction in plaque macrophage content and to subendothelial accumulation of invaded macrophages.

A second striking hallmark of Hck/Fgr deficiency in atherosclerosis was the paradoxical induction of necrotic core expansion and lesion vulnerability, with reduced fibrosis, SMC accumulation, and collagen deposition. This phenotype is remarkably similar to that observed in ear excision wounds treated with Src tyrosine kinase inhibitors,[31] alluding to a positive role of Hck/Fgr in macrophage profibrotic functions. Compatible with the latter, conditioned medium from dKO macrophages was seen to reduce collagen production by vascular SMC. The impact of this plaque-destabilizing effect

will be considerably augmented by the increased retention of extravasated, migration-defective dKO monocytes in subendothelial tissue close to the fibrous cap, where they can exert their cap-erosive functions.

Our experiments thus underpin the importance of Hck/Fgr not only in migration, but also in macrophage profibrotic differentiation. Analysis of microarray data sets and our gene expression studies point to divergent regulation of Hck and Fgr expression in response to macrophage classical and alternative polarization, supportive of a role for these kinases in the spectrum of macrophage immune differentiation. However, we did not observe consistent Hck/Fgr deficiency–associated shifts in macrophage polarization marker expression, but Hck/Fgr-deficient macrophage displayed functional changes relevant to plaque stability, with inhibited SMC extracellular matrix protein deposition and reduced efferocytosis capacity as the most prominent features.

In conclusion, Hck and Fgr deficiency is associated with a reduced recruitment of myeloid cells to the plaque, despite the observed skewing of monocytes toward the proinflammatory Ly-6C^{hi} monocytes. However, the beneficial effects of reduced leukocyte influx are counteracted by the focal retention of extravasated monocytes in the fibrous cap, promoting its erosion and plaque vulnerability. The apparent profibrotic function of Hck/Fgr raises a note of caution against the use of Src kinase inhibitors for the treatment of atherosclerosis, where reduced macrophage accumulation and fibrous cap integrity are desired to attain a stable plaque profile. However, their novel application as antifibrotic therapy in systemic sclerosis[32,33] and our results support their potential to treat fibroblastic vasculopathies such as restenosis and disorders where the simultaneous reduction of fibrosis and macrophage accumulation are desired.

Acknowledgments

We thank M Waqar Aslam for technical assistance with opsonized particle phagocytosis assays and TRI (Toulouse Réseau Imagerie) and Anexplo GenoToul facilities at the IPBS (Toulouse). We also thank Dr Lowell (University of California, San Francisco, CA) who kindly provided the Hck/Fgr-deficient mice.

Sources of Funding

This work was supported in part by the Netherlands Organization for Scientific Research (# 912.02.037, to Dr Medina; grant 916.86.046, to Dr Bot; grant 91712303, Dr Soehnlein), by the Netherlands Heart Foundation (grant D2003T201, to Drs Biessen and de Jager), by the European Community's Seventh Framework Program under grant agreement HEALTH-F4-2011 to 282095 (to Drs Cougoule and Maridonneau-Parini), by the Agence Nationale de la Recherché (grant 2010-01301; to Drs Cougoule and Maridonneau-Parini), by the Fondation pour la Recherche Médicale (DEQ 20110421312; to Drs Cougoule and Maridonneau-Parini), by the European Union (TARKINAID project; grant 282095 (to Dr Mócsai), and by the DFG (SO876/6-1, SFB914 TP B08, SFB1123 TP A6 and B5; to Dr Soehnlein). Dr Biessen is Established Investigator of the Netherlands Heart Foundation (D2003T201); Dr Mócsai is a Senior Research Fellow of the Wellcome Trust (grant 087782).

Disclosures

None.

References

1. Murray PJ, Wynn TA. Protective and pathogenic functions of macrophage subsets. *Nat Rev Immunol*. 2011;11:723–737. doi: 10.1038/nri3073.
2. Ley K, Laudanna C, Cybulsky MI, Nourshargh S. Getting to the site of inflammation: the leukocyte adhesion cascade updated. *Nat Rev Immunol*. 2007;7:678–689. doi: 10.1038/nri2156.
3. Rikitake Y, Takai Y. Directional cell migration regulation by small G proteins, nectin-like molecule-5, and afadin. *Int Rev Cell Mol Biol*. 2011;287:97–143. doi: 10.1016/B978-0-12-386043-9.00003-7.
4. Muller WA. Mechanisms of leukocyte transendothelial migration. *Annu Rev Pathol*. 2011;6:323–344. doi: 10.1146/annurev-pathol-011110-130224.
5. Yago T, Shao B, Miner JJ, Yao L, Klopocki AG, Maeda K, Coggeshall KM, McEver RP. E-selectin engages PSGL-1 and CD44 through a common signaling pathway to induce integrin alphaLbeta2-mediated slow leukocyte rolling. *Blood*. 2010;116:485–494. doi: 10.1182/blood-2009-12-259556.
6. Zarbock A, Abram CL, Hundt M, Altman A, Lowell CA, Ley K. PSGL-1 engagement by E-selectin signals through Src kinase Fgr and ITAM adapters DAP12 and FcR gamma to induce slow leukocyte rolling. *J Exp Med*. 2008;205:2339–2347. doi: 10.1084/jem.20072660.
7. Baruzzi A, Caveggion E, Berton G. Regulation of phagocyte migration and recruitment by Src-family kinases. *Cell Mol Life Sci*. 2008;65:2175–2190. doi: 10.1007/s00018-008-8005-6.
8. Harb D, Bujold K, Febbraio M, Sirois MG, Ong H, Marleau S. The role of the scavenger receptor CD36 in regulating mononuclear phagocyte trafficking to atherosclerotic lesions and vascular inflammation. *Cardiovasc Res*. 2009;83:42–51. doi: 10.1093/cvr/cvp081.
9. Hilgendorf I, Eisele S, Remer I, Schmitz J, Zeschky K, Colberg C, Stachon P, Wolf D, Willecke F, Buchner M, Zirlik K, Ortiz-Rodriguez A, Lozhkin A, Hoppe N, von zur Muhlen C, zur Hausen A, Bode C, Zirlik A. The oral spleen tyrosine kinase inhibitor fostamatinib attenuates inflammation and atherogenesis in low-density lipoprotein receptor-deficient mice. *Arterioscler Thromb Vasc Biol*. 2011;31:1991–1999. doi: 10.1161/ATVBAHA.111.230847.
10. Katsume A, Okigaki M, Matsui A, Che J, Adachi Y, Kishita E, Yamaguchi S, Ikeda K, Ueyama T, Matoba S, Yamada H, Matsubara H. Early inflammatory reactions in atherosclerosis are induced by proline-rich tyrosine kinase/reactive oxygen species-mediated release of tumor necrosis factor-alpha and subsequent activation of the p21Cip1/Ets-1/p300 system. *Arterioscler Thromb Vasc Biol*. 2011;31:1084–1092. doi: 10.1161/ATVBAHA.110.221804.
11. Shah Z, Kampfrath T, Deiuliis JA, Zhong J, Pineda C, Ying Z, Xu X, Lu B, Moffatt-Bruce S, Durairaj R, Sun Q, Mihai G, Maiseyeu A, Rajagopalan S. Long-term dipeptidyl-peptidase 4 inhibition reduces atherosclerosis and inflammation via effects on monocyte recruitment and chemotaxis. *Circulation*. 2011;124:2338–2349. doi: 10.1161/CIRCULATIONAHA.111.041418.
12. Berton G, Mócsai A, Lowell CA. Src and Syk kinases: key regulators of phagocytic cell activation. *Trends Immunol*. 2005;26:208–214. doi: 10.1016/j.it.2005.02.002.
13. Cougoule C, Le Cabec V, Poincloux R, Al Saati T, Mège JL, Tabouret G, Lowell CA, Laviolette-Malirat N, Maridonneau-Parini I. Three-dimensional migration of macrophages requires Hck for podosome organization and extracellular matrix proteolysis. *Blood*. 2010;115:1444–1452. doi: 10.1182/blood-2009-04-218735.
14. Bhattacharjee A, Pal S, Feldman GM, Cathcart MK. Hck is a key regulator of gene expression in alternatively activated human monocytes. *J Biol Chem*. 2011;286:36709–36723. doi: 10.1074/jbc.M111.291492.
15. Lowell CA. Src-family and Syk kinases in activating and inhibitory pathways in innate immune cells: signaling cross talk. *Cold Spring Harb Perspect Biol*. 2011;3:. doi: 10.1101/cshperspect.a002352.
16. Cougoule C, Carréno S, Castandet J, Labrousse A, Astarie-Dequeker C, Poincloux R, Le Cabec V, Maridonneau-Parini I. Activation of the lysosome-associated p61Hck isoform triggers the biogenesis of podosomes. *Traffic*. 2005;6:682–694. doi: 10.1111/j.1600-0854.2005.00307.x.
17. Sambrook J, Russell DW. Extraction, purification and analysis of mRNA from eukaryotic cells. In: Argentine J, Irwin N, Janssen KA, Curtis S, Zierler M, eds. *Molecular Cloning: A Laboratory Manual*. Cold Spring Harbor, NY: Cold Spring Harbor Laboratory Press; 2001:7.4–7.9
18. Fuentes-Duculan J, Suárez-Fariñas M, Zaba LC, Nograles KE, Pierson KC, Mitsui H, Pensabene CA, Kzhyshkowska J, Krueger JG, Lowes MA. A subpopulation of CD163-positive macrophages is classically activated in psoriasis. *J Invest Dermatol*. 2010;130:2412–2422. doi: 10.1038/jid.2010.165.
19. Hatakeyama S, Iwabuchi K, Ogasawara K, Good RA, Onoé K. The murine c-fgr gene product associated with Ly6C and p70 integral membrane

protein is expressed in cells of a monocyte/macrophage lineage. *Proc Natl Acad Sci U S A*. 1994;91:3458–3462.
20. Tacke F, Alvarez D, Kaplan TJ, Jakubzick C, Spanbroek R, Llodra J, Garin A, Liu J, Mack M, van Rooijen N, Lira SA, Habenicht AJ, Randolph GJ. Monocyte subsets differentially employ CCR2, CCR5, and CX3CR1 to accumulate within atherosclerotic plaques. *J Clin Invest*. 2007;117:185–194. doi: 10.1172/JCI28549.
21. Van Goethem E, Poincloux R, Gauffre F, Maridonneau-Parini I, Le Cabec V. Matrix architecture dictates three-dimensional migration modes of human macrophages: differential involvement of proteases and podosome-like structures. *J Immunol*. 2010;184:1049–1061. doi: 10.4049/jimmunol.0902223.
22. Van Goethem E, Guiet R, Balor S, Charrière GM, Poincloux R, Labrousse A, Maridonneau-Parini I, Le Cabec V. Macrophage podosomes go 3D. *Eur J Cell Biol*. 2011;90:224–236. doi: 10.1016/j.ejcb.2010.07.011.
23. Wiesner C, Le-Cabec V, El Azzouzi K, Maridonneau-Parini I, Linder S. Podosomes in space: macrophage migration and matrix degradation in 2D and 3D settings. *Cell Adh Migr*. 2014;8:179–191.
24. Murphy DA, Courtneidge SA. The 'ins' and 'outs' of podosomes and invadopodia: characteristics, formation and function. *Nat Rev Mol Cell Biol*. 2011;12:413–426. doi: 10.1038/nrm3141.
25. Swirski FK, Libby P, Aikawa E, Alcaide P, Luscinskas FW, Weissleder R, Pittet MJ. Ly-6Chi monocytes dominate hypercholesterolemia-associated monocytosis and give rise to macrophages in atheromata. *J Clin Invest*. 2007;117:195–205. doi: 10.1172/JCI29950.
26. Robbins CS, Swirski FK. The multiple roles of monocyte subsets in steady state and inflammation. *Cell Mol Life Sci*. 2010;67:2685–2693. doi: 10.1007/s00018-010-0375-x.
27. Combadière C, Potteaux S, Gao JL, Esposito B, Casanova S, Lee EJ, Debré P, Tedgui A, Murphy PM, Mallat Z. Decreased atherosclerotic lesion formation in CX3CR1/apolipoprotein E double knockout mice. *Circulation*. 2003;107:1009–1016.
28. Cheng C, Tempel D, van Haperen R, de Boer HC, Segers D, Huisman M, van Zonneveld AJ, Leenen PJ, van der Steen A, Serruys PW, de Crom R, Krams R. Shear stress-induced changes in atherosclerotic plaque composition are modulated by chemokines. *J Clin Invest*. 2007;117:616–626. doi: 10.1172/JCI28180.
29. Martínez-Hervás S, Vinué A, Núñez L, Andrés-Blasco I, Piqueras L, Real JT, Ascaso JF, Burks DJ, Sanz MJ, González-Navarro H. Insulin resistance aggravates atherosclerosis by reducing vascular smooth muscle cell survival and increasing CX3CL1/CX3CR1 axis. *Cardiovasc Res*. 2014;103:324–336.
30. Ridley AJ. Life at the leading edge. *Cell*. 2011;145:1012–1022. doi: 10.1016/j.cell.2011.06.010.
31. Sun X, Phan TN, Jung SH, Kim SY, Cho JU, Lee H, Woo SH, Park TK, Yang BS. LCB 03-0110, a novel pan-discoidin domain receptor/c-Src family tyrosine kinase inhibitor, suppresses scar formation by inhibiting fibroblast and macrophage activation. *J Pharmacol Exp Ther*. 2012;340:510–519. doi: 10.1124/jpet.111.187328.
32. Skhirtladze C, Distler O, Dees C, Akhmetshina A, Busch N, Venalis P, Zwerina J, Spriewald B, Pileckyte M, Schett G, Distler JH. Src kinases in systemic sclerosis: central roles in fibroblast activation and in skin fibrosis. *Arthritis Rheum*. 2008;58:1475–1484. doi: 10.1002/art.23436.
33. Beyer C, Distler O, Distler JH. Innovative antifibrotic therapies in systemic sclerosis. *Curr Opin Rheumatol*. 2012;24:274–280. doi: 10.1097/BOR.0b013e3283524b9a.

CLINICAL PERSPECTIVE

Atherosclerosis, a major underlying cause for cardiovascular disorders is a chronic lipid-driven inflammatory disease that is impacted by many risk factors: hypertension, dyslipidemia, type 2 diabetes mellitus, etc. Current drug therapy appears to reduce the risk of future cardiovascular events in 30% of patients, urging for new complementary medication to also reduce risk in poorly responding patients. It is in this context that inflammation has been embraced as a potential target for intervention. In particular, the accumulation and activity in atherosclerotic plaque of potentially deleterious leukocyte subsets have so far been investigated for their effectiveness to quench plaque inflammation and improve its stability, both in preclinical and, albeit with little success, in clinical studies. In this study, we have interrogated the therapeutic potential of inhibition of the mobility of plaque macrophages, the abundant presence of which is viewed as a hallmark of the vulnerable plaque. We are the first to show that hyperlipidemic mice with blunted expression of 2 drugable regulators of phagocyte mobility (the kinases Hck and Fgr) have smaller plaques, which paradoxically display clear features of increased vulnerability, such as thinned fibrous caps. We were able to demonstrate that this may be caused by trapping newly invaded phagocytes in the fibrous cap region, creating a lytic milieu that will affect focal erosion. Our findings thus raise a note of caution regarding the therapeutic value of Hck and Fgr as key targets for intervention in plaque inflammation.